International Journal of Scientific Research in Engineering and Management (IJSREM)
Volume: 09 Issue: 05 | May - 2025 SJIF Rating: 8.586 ISSN: 2582-3930

Environmental Data Analytics for air Quality Monitoring

Rajmohan Soni, Dr Vishal Shrivastava, Dr. Ashok Kumar Kajla

Rajmohansoni0512@gmail.com, vishalshrivastava.cs@aryacollege.in, ashokkajla@aryacollege.in

[a]Department of Artificial Intelligence and Data Science, Student of Artificial Intelligence and Data Science,

Arya College of Engineering and IT, Kukas, Jaipur

KEYWORDS

Air pollution sensing; Air sensor/monitor performance, Low-cost sensor/monitor; Personal exposure monitoring; Sensor data utilisation

ABSTRACT

This paper presents a network for indoor and outdoor air quality monitoring. Each node is installed in a different room and includes tin dioxide sensor arrays connected to an acquisition and control system. The nodes are hardwired or wirelessly connected to a central monitoring unit. To increase the accuracy of gas concentration measurement and prevent false alarms, two gas sensor influence quantities, namely temperature and humidity, are also measured. Advanced processing based on multiple input single-output neural networks are implemented at the network sensing nodes to get temperature and humidity compensated gas concentration values. The anomalous operation of the network sensing nodes and power consumption are also discussed. Index Terms—Air quality (AirQ), embedded Web server, neural network, wireless networks.

1 INTRODUCTION

Air is critical for our survival as it contains the oxygen that we need for breathing. Although air is composed of greater than 99.9% of nitrogen, it can be argon, oxygen, argon, inert gases as well as water vapor, and it is good and essential for every form of life. Human activities contribute harmful substances in the air which can cause danger to plants, animals and humankind as well.

The amount of pollution inhaled in the air can be measured in terms of the carbon monoxide (Co), sulphur dioxide, nitrogen dioxide and ozone levels in the air. The European Environment Agency has set minimum limit levels for these harmful substances which are 10, 350, 40, and 120 microgrammes per meter cube respectively.

Also in the indoor environment pollution has to be solved for example in our homes, workplaces, in offices and educational centers with the children. Also, some of these pollutants can be caused indoors when smoking and cooking for instance is done. In most of the developed countries, around 80 - 90 percent of time of population is spent indoors thus increasing exposure to domestic air particles. The certain determination of temperature, carbon monoxide (CO) levels and humidity are standard approaches of assessing indoor space. Even in the aggregate, these data sets do not enable one to make a good indoor air characterization. The emergence of WLAN technology together with the introduction of cheap Linksys WAP11 active points units manufactured Panostal Dry, Wireless Local Area PANs(networks) revolutionized the wireless industry For instance 11 g wireless solutions such as D link and Cardbus as well bridges like DW 810 has the potential of deploying indoor and outdoor air monitoring networks which are cost effective and have great suitabilitY and modularity.

Tin oxide –e.g. Tin oxide cheap gas senors such as Fargoro, and Nemoto 3 Regis are gas limited. To ease some of their cross sensitivities limitations and temperature and humidity dependence, prima data preprocessing is needed.

The objective of this paper is to describe a tin oxide coupled multilayer Wi-Fi indoor-outdoor air quality tele-monitoring system that enables to accurately measure air quality and detect air pollution events and abnormal operation.

International Journal of Scientific Research in Engineering and Management (IJSREM)
Volume: 09 Issue: 05 | May - 2025 SJIF Rating: 8.586 ISSN: 2582-3930

1 DIRECT AND INVERSE MODELING OF THE SENSORS'CHARACTERISTICS

The nonlinearity of the sensors requires the usage of direct and inverse modeling in the sensor calibration and on-line measurement phase [7]. For the specific case of tin oxide gas sensors TGS800, TGS822, TGS842, and TGS203, the response of the sensors is significantly affected by parameters like temperature, humidity, and cross influence of the other gases. For practical and economical reasons, the number of calibration points is very low, and thus, a neural network (multilayer perceptron architecture), which is a global approximator of multivariable characteristics [8], was used in this paper. Polynomial modeling is another solution for multivariable characteristics modeling.

Representative of this type of solution is the polynomial model that is a part of the IEEE1451.2 standard for smart sensors particularly related to smart sensors correction engine implementation [9]. The method represents an interesting solution.

However, it requires a large set of data (i.e., a higher number of calibration points compared with a neuronal network model) for polynomial model coefficients calculation [10], i.e. where Xn are the input variables to the sensor characteristic block, Hn are the offsets to the input variables, and the D(k) represents the degree of the input Xk, i.e., the highest power to which [Xk −Hk] is raised in any term of the multinomial.The Ci,j,.,p represent the calculated correction coefficients for each term values that are obtained, considering the segmentation of the input variable range. The accuracy of the method is dependent on the polynomial degree, the number of segments, and the number of values included in defined subranges that make the multivariable polynomial inverse modeling for external factors compensation computationally expensive. Considering only one segment for a given gas concentration, where the voltage acquired from gas sensor channel represents the primary variable (X1 = VGi), and the number of impact factors on gas concentration measuring limited to temperatures and humidity expressed through the voltage values obtainedfrom temperature and relative humidity sensor channels (X2 = VT,X3 = VRH), and compensated values of gas concentrations. From here, it follows that in order to diminish complexity the first-degree polynomial approximation is considered. Higher accuracy can that with a higher degree multivariable polynomial model, which of course involves an increase in the computational load. Comparing the "classical" polynomial modeling with neural network modeling indicates that the number of calibration points used for the computation of the coefficients of the polynomial for the given accuracy of inverse characteristic modeling is usually larger than the number of calibration points utilized for design the neuronal network sensor models [11]. Moving the complex processing from the embedded server to the Web browser side permits us to overcome some of the drawbacks of neuralnetwork processing such as the high number of multiplication and the use of nonlinear transfer functions (e.g., tanh()).

2 SENSORS'NETWORK

Gas sensor networks present a promising way of extracting information from the monitored regions. The following two types of WLAN architectures were considered:

1) an ad hoc architecture and 2) an AP infrastructure network, which guarantees additional services (e.g., data publishing on the wired Internet), keeping in mind that the AP operates like a bridge between the wired and wireless network [12]. The Ad hoc architecture seems to be a good solution, especially for air quality monitoring in outdoor conditions because of reduced numbers of elements and thus lower power consumption. The ad hoc smart sensor network (Fig. 1, case 1) comprises the following three elements: 1) PC with an IEEE802.11g-compatible Wi-Fi cardbus adapter (DWL-G650+) as the primary control and processing unit; 2) a set of sensing nodes (SNj) with air quality sensors (GS1,GS2,.,GSi); and 3) a data acquisition, primary processing, and transmission control protocol/Internet protocol (TCP/IP) communication unit (APC) based on IPµ8930 general-purpose network controller whose Ethernet port is connected to a DWL-G810 wireless bridge. Referring to the AP infrastructure (case 2), the wireless network node components are the same as that of case 1, with the only difference is that it contains an AP (LinksysWAP11), which is a component that expands the wireless subnetwork range capabilities and allows wireless network traffic to be transmitted over the wired network that may incorporate extrawired sensing nodes (SNj) deployed in various rooms (Rwjrooms;
Fig. 2).

A few key benefits of the adoption of sensor networks are cost-effectiveness, scalability, and community engagement via an open data platform. In this regard, cheap sensors could cover diverse terrains to provide quality data on air for policymakers and even the public. However, challenges abound. Low-cost sensors frequently have to be calibrated and validated, which may compromise accuracy.

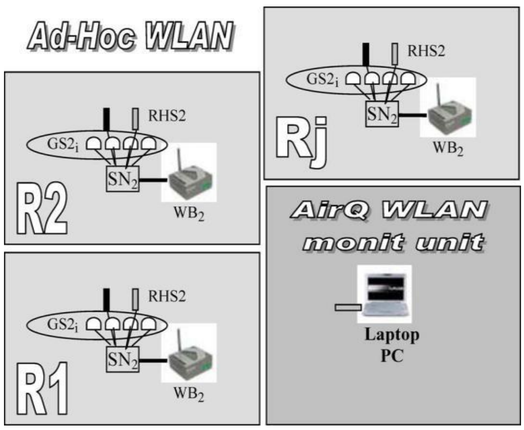

Fig. 1. Air quality smart sensor network ad hoc architecture associated with different rooms (R1, R2, Rj), where SNj are sensing nodes, GSji are gas sensors, TSj are the temperature sensors, RHSj is the relative humidity sensor and WBj are wireless bridges.

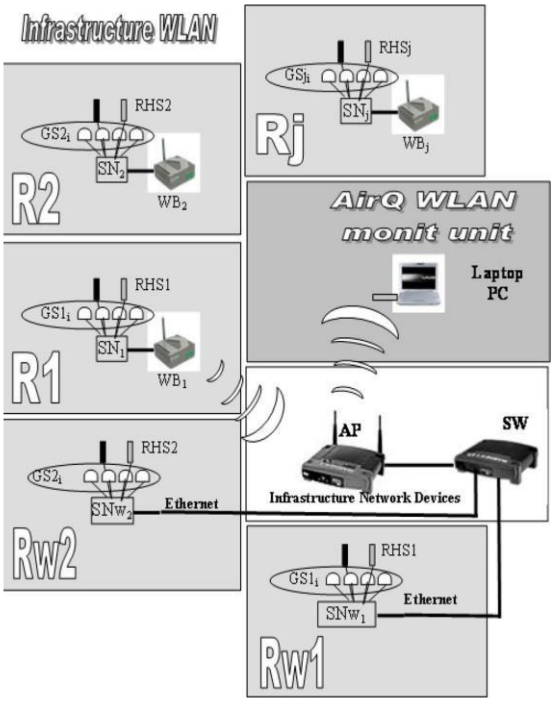

Figure 2. Architecture of an infrastructure WLAN air quality smart sensor network That contains the sensor deployed in the different rooms. R1, Rj: Rooms With wireless sensing nodes. Rw1 and Rw2: Rooms with wired sensing nodes.SNj: Sensor's nodes. GSji: Gas sensors. TSj: Thermometers. RHSj: Relative humidity sensors. WBj: Wireless bridges. AP: Access point.

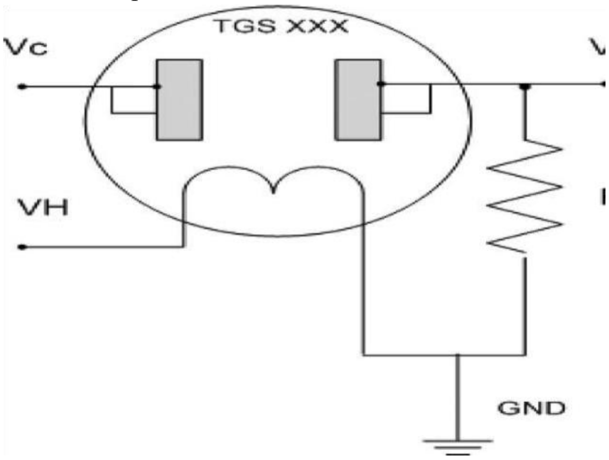

Fig. 4. Gas sensor conditioning circuit. Vc: Circuit voltage. VH: Heater voltage. VGS: Gas sensor output voltage. RL: Load resistance.

range capabilities and allows to transfer wireless network traffic over the wired network that can be equipped by additional wired sensing nodes SNj distributed in different rooms Rwjrooms; Fig. 2

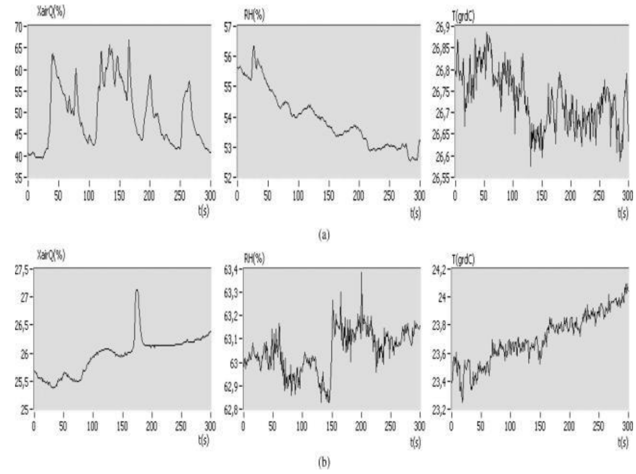

A. Sensing Nodes

The sensing nodes are designed and implemented for performing air quality (AirQ) monitoring using low-cost gas sensors and, at the same time, getting the extra information about the temperature T and relative humidity RH. In this way, the concentration measurements of these gases can be performed more precisely by increasing the accuracy while using error compensation caused by temperature and humidity influence.

monitoring of air quality possible. The future of this evolving technology will continue to be more efficient,accessible, and versatile, driving innovation in the monitoring and analytics of environmental data.

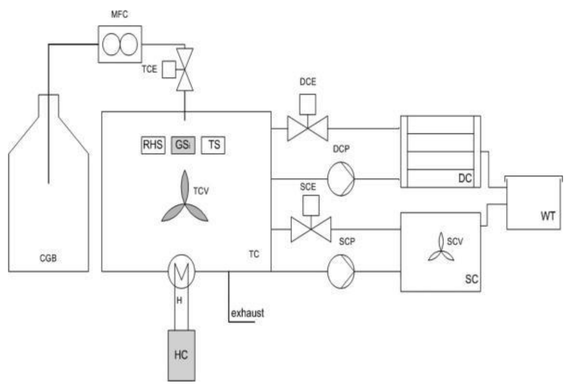

Used gas sensors are sintered using SnO2 semiconductor.

heated sensors provided by Figaro [13] that ensure the detection of the pollution event (TGS800general air contaminant sensor-AC), methane (TGS842-M), alcohol and organic solvent (TGS822SV), and CO (TGS203-CO). Data on temperature and relative humidity are obtained with Smartec SMT160-30 [14] and Humirel HM1500 [15] temperature and relative humidity transducers, respectively. The experimental direct characteristics of the sensor are explained by voltages obtained at the gas sensor conditioning circuit.

Output for various concentrations of gas, in parts per million. The conditioning circuit for air pollution sensor TGS800, solvent vapors sensor TGS822 and the methane sensor TGS842 as used is shown in Fig. 4. In order to characterize the sensor, each of the considered gas sensors (GSi) is individually introduced in a test chamas part of a laboratorydeveloped gas sensor calibrationsystem. The values of gas concentration are imposed using a mass flow controller (MC Alicat Scientific) connected to gas bottles with standard concentration (e.g., 100 ppm CO).Temperature and humidity are measured using the temperature and relative humidity sensors that are also incorporated in thechamber. Various values of temperature and relative humidity are applied to with a series of drying and saturation chambersthat are connected to the test chamber and air pumps (Fig. 5).The drying chamber with two Peltiercells is connected to the test chamber to lower the humidity. After condensation on the Peltier cells surface, the condensed liquid in the drying chambers collected and pumped off from the drying chamber. Low this is how values of relative humidity can be obtained in this manner (e.g.,RH =20%). Higher humidity values are obtained when thesaturation chamber is connected to the testing chamber. In thiscase, condensed/distilled water is pumped from the water tankand vaporized into the air circulation system. Values of 95% were reached using this procedure. Using the RH variation procedure, gas sensors characteristics for RH1 = 35%, RH2 =65% and RH3 = 95% were obtained.

Temperature A Peltier cell is applied. Additionally, there is a testing chamber ventilator for forcing cold or warming up air in the testing chamber. In the case to be tested, several temperature values are set, T1 =10◦C, T2 =15◦C; T3 =20◦C, T4 =25◦CandT5
=30◦C. A gas exhaust circuit is applied for the testing chamber cleaning after specific testing of one type of gas sensor (e.g., TGS842 Methane gas sensor).

Sensing nodes are the building blocks of sensors' networks and, hence, very key to environmental data analytics in monitoring air quality. All sensing nodes are compactly designed autonomous systems that encompass all hardware and software requirements to measure, process, and transmit environmental data. These nodes are specifically deployed to monitor various air quality parameters with realtime and spatially distributed data critical to understand and mitigate air pollution.

The core of the modern air quality monitoring systems lies in sensing nodes that deliver the required environmental data to be used in analytics. Advanced sensing technologies coupled with solid communication and processing capabilities within sensing nodes make real-time distributed, actionable Fig. 5. Gas sensor calibration system architecture. CGB: Calibration gas bottle. MFC: Mass flow control. TCE: Testing chamber electrovalve. DCE: Drying chamber electrovalve. SC: Saturation chamber electrovalve. DCP: Drying chamber pump. SCP: Saturation chamber pump. DC: Drying chamber. SC: Saturation chamber. HC: Heater control. H: Heater. WT: Water tank. TCV: Testing chamber ventilator. SCV: Saturation chamber ventilator.

values of temperature were given, T1 =10◦C, T2 =15◦C;T3 =20◦C, T4 =25◦CandT5 =30◦C.

The gas exhaust circuit is used for cleaning the testing chamber. After a specific gas sensor test, for example, TGS842 Methane gas sensor testing.

B. APC

Applied are the voltages obtained from sensors' channels to the analog inputs of a general-purpose network controller and Web server (Ipsil IPμ8930). It performs sensing channels data conversion-the voltage is converted in parts per million for a particular gas, in degrees in the Celsius scale for the other, and in percent, on the otherhand. Conversion is done for Webdata publishing (case 1) or transmission, using TCP/IP.

Communication to the main processing and control unit (laptopPC) that performs the data logging, data processing, and Web publishing through a LabVIEW Web server (case 2).

3 DATA PROCESSING

Two types of sensor data processing architectures that allow the calculation of several air quality values are implemented using JavaScript and LabVIEW Web publisher technologies. The first one is a neural network algorithm implemented in JavaScript in the embedded server (Web sensor) and represents one of the main novelties of the work. The second software architecture is implemented in the network PC and performs the following three operations: 1) data reading coming from sensing nodes by remote control over TCP/IP; 2) detection of air pollution events and estimation of gas concentration on the basis of neural network inverse models of gas sensors; and 3) logging and publishing on the Web of data characterizing air quality. Such architecture was realized making use of facilities provided by LabVIEW.

JavaScript is bound with the smart sensor network and Guarantees dynamic independent generation of web pages. The SNj sensor nodes, sustained by the architectures of embedded Web servers, take and treat the voltages coming out from the sensors' channels through a set of JavaScript functions, JSi that are implemented within the HTML file stored in an embedded Web server, Ipsil IPμ8930, whose electrically erasable programmable read-only memory EEPROM. JSi complexity depends on the sensor it is assigned to. Data processing is performed mainly at the Web browser level, which reduces the computational load associated with embedded Web servers and is also important as regard power consumption and Web server autonomy.

The utilization of NPBs is related with the inverse modeling of gas sensor multivariable nonlinear characteristics, which are strongly dependent on temperature and humidity but are also influenced by the concentration of other gases as part of the analyzed gas mixture.

International Journal of Scientific Research in Engineering and Management (IJSREM)
Volume: 09 Issue: 05 | May - 2025 SJIF Rating: 8.586 ISSN: 2582-3930

The concentrations of the analyzed gas mixture are determined. Based on designed NPBi, a digital readout of the gas concentration with temperature and compensation is acquired .

A. NPB Architecture and Design

The used neural processing blocks (NPBi) are two inputs-one output multilayer perceptron neural networks (Fig. 6)

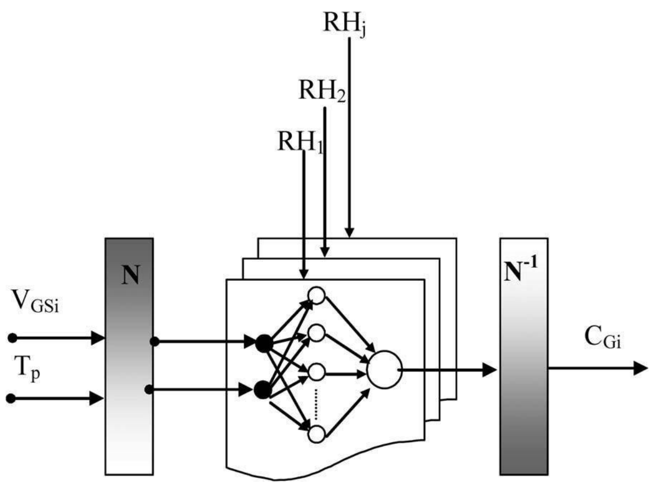

Fig.6. TheNPBiarchitecture.N, N−1: Normalization and denormalization blocks. RHj: Humidity selector.CGi: Temperature and humidity compensated values of the gas concentrationGi.TP:Temperatureinputvalue.VGSi :Input voltagevalueontheGSichanne.

The internal parameters of the NPBi (weights and biases) are calculated offline by MATLAB. The neural network training data were obtained in the system calibration phase. They are voltage values(VGSi) acquired from the gas concentration measurement channel for different values of gas concentration CGi and different temperature (Tp) and relativehumidity (RHi) conditions.

The developed MATLAB neural network design program calculates different sets of weights and biases for each RHi experimental value(e.g.,RH= 45%,55%,65%. In the air quality parameters measuring phase, the calculated weights are used by JavaScript- or LabVIEW-implemented functions for online processing of the acquired voltages.

Because GSi characteristics depend on humidity,an accure measurement of the gas concentration is provided using different NPBiRHs whose weights and biasesare calculated using data obtained for different relative humidity conditions (i.e.RH=45%,55%, and 65%)and the interpolation method presentedin.

The number of layers in NPBi is three. The hidden layers contain two to five tansignoid (tansig(x)) neurons, while the output layer contains one linear (l(x)) neuron. This reduces the computational load.

Two design criteria for NPBi: the type of neurons, and the quantity of them in the hidden layer which determines its ability to be adapted to a certain characteristic.

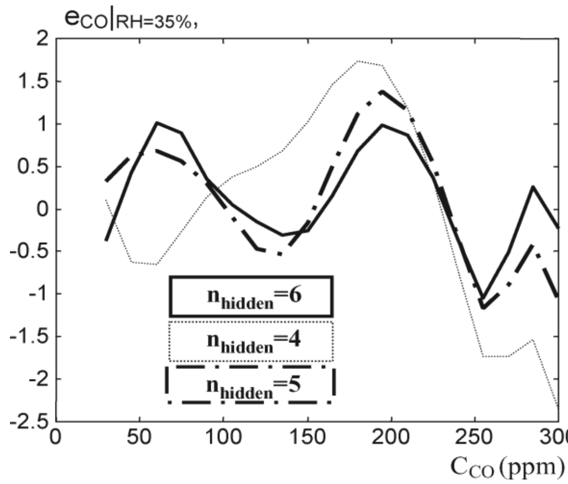

Fig. 7. Modeling error versus concentration for different NPB_{CO} architectures (T = 10°C).

The requirement for different memory space and processing capabilities in hardware platforms varies from one type of nonlinear activation function to another. In this paper (tansignoid activation function), the neural processing task is distributed between the sensing node, which comprises an embedded Web server, and the Web client, which is the laptop PC, thus reducing the complex processing requirements at the IPµ8930 level. In this work, having taken into account the memory space of the IPµ8930, an optimization in terms of the HTML number of pages and page size was also performed simultaneously. A study on the necessary number of neurons in relation to a required NPBi performance, expressed in a modeling error, has been conducted to reduce vector weights and biases sizes. More neurons mean complex processing but, above all, large dimensions of the weights and biases matrices, meaning large memory requirements.

Therefore, the number of hidden neurons was to be reduced, and the memory resources of the IPµ8930 (512 kB EEPROM) and the ability of the browser to process online sensor data were taken into account. In the case of the specific CO measuring channel, the training set contains, as a target, 15 values of CO concentration uniformly distributed in the 30–300 ppm interval.

The input values are the voltage values obtained from the TGS203 CO concentration measuring channel corresponding to the concentrations mentioned above.

The temperature in the testing chamber was measured to be Tp [in degrees Celsius] = 10 × p, p = {1,2,3,4,5}, and relative

International Journal of Scientific Research in Engineering and Management (IJSREM)
Volume: 09 Issue: 05 | May - 2025 SJIF Rating: 8.586 ISSN: 2582-3930

humidity was RH = 35%. The weights and biases (i.e., WNPBi and BNPBi) of the neural network were calculated by using the Levenberg–Marquardt algorithm.

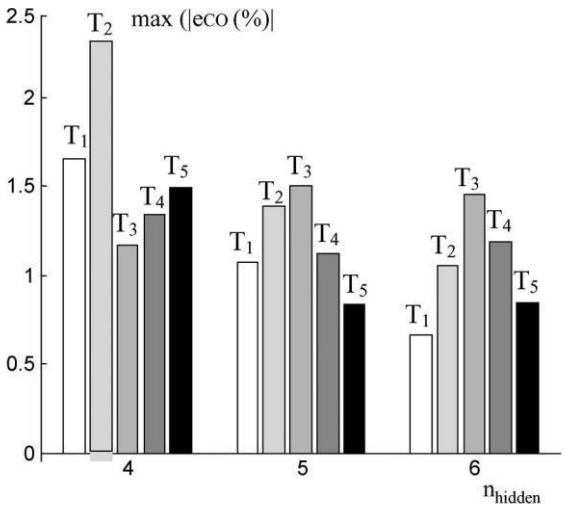

Fig.8.MaximuminversemodelingerrorfordifferentN PBCOarchitectures(nhidden={4,5,6})and different temperatures Tp=10p◦C.

As the used gas sensors character in respect to temperature is, obviously related with CO channel modelling error study versus temperature has been done (Fig. 8).

Since humidity is the influencing quantity, the characteristics of primary gas selectivity are different for different values of relative humidity and hence, the gas concentration measurement accuracy is also different. Hence, experimental data obtained for three different values of relative humidity, i.e., RH1 = 35%, RH2 = 65%, and RH3 = 95% and five values of temperatures included in the IT = [10;50]◦C were considered. The values of imposed concentrations of gases for the tests on the measurement system were: ten values of methanol concentration distributed in ICM = [500;5000] ppm and 15 values of carbon monoxide concentration ICCO = [30;300] ppm, and 15 values of solvent vapors or ethanol vapors concentration, which was CSV = [50;5000] ppm.

Based on GSi voltages for considered gases concentrations, taking temperature and humidity into account, three sets of weights and biases were calculated for measurement channel of CO, methane, and solvent vapor at 35%, 65%, and 95% relative humidity, respectively.

B. NPB$_i$ JavaScript Implementation The weights and biases data are stored in numerical arrays used by the JavaScript neural processing functions JSNAC, JSNM, JSNCO, and JSNSV that are embedded in the APC's HTML pages.

The implementation of JSN uses JavaScript arithmetic operators and the JavaScript "exp" method of the JavaScript Math object. Other implemented functions perform the sums associated with the calculation.

The method applied to transmit data from the APC to the JavaScript functions as portions of the HTML pages stored in the memory of the AirQ node relies on the IPμ8930 dynamic WebHoles feature [20]. Therefore, with every access made by the PC browser of the given HTML page (e.g., 70_AirQ_G.htm) to the IPμ8930 Web server (e.g., http://193.136.143.205/70_AirQ_

G.htm), the decimal code DACHj correlated with measuring channel j voltage, ACHj (such as 625 code corresponding to VGsi =
3 V) is entered into dynamically configured WebHole (which was pre-configured by IPμ8930 WebHole Editor). Inputting the preset sequence of the digits "00000" (after which DACHj had been replaced using dynamic WebHoles technique) into the JSN acquires calculated values of gas concentration. The JST and the JSRH also utilize dynamic WebHoles for computation of RH and T.

V. DATA PUBLISHING

The air quality data at each sensing node are published using APC Web server capabilities and APC–laptop PC TCP/IP communication, together with PC LabVIEW Web server capabilities.

A. APC Web Server Publishing

The capabilities of the APC Web server permit the laptop PC in the network to access dynamic web pages related to the present values of the concentrations of the gases using the browser, like Internet Explorer. Thus, each APC in the network holds the main page of the distributed air quality monitoring system, such as it is presented at Fig. 9, which contains a collection of hyper-links called sensing node i, such as sensing node 2. For each sensing node, temperature in degrees Celsius, percent relative humidity, and the air quality index in XAirQ are shown.

The air quality index is defined as the ratio of V _AirQ, that is, the voltage value found in the air quality sensor channel, to the value denoting the clean air condition, namely no pollution, (V_pal, in volts) by which the air quality level is measured (XAirQ = 100% for no pollution, and XAirQ = 0% for extreme air pollution).

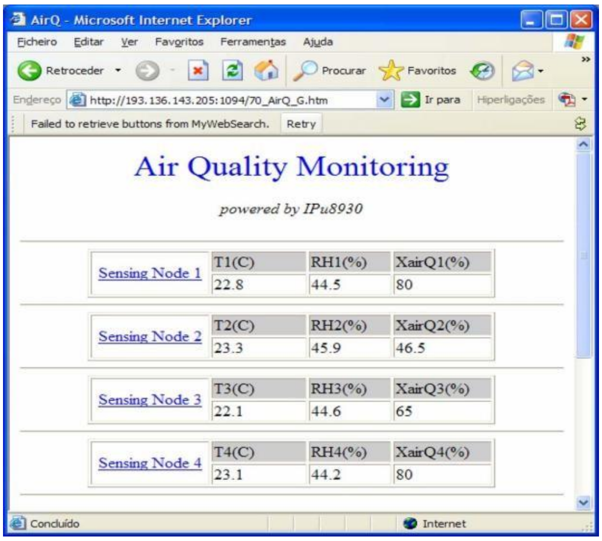

Fig. 9. Air quality monitoring webpage [T_i (in degrees Celsius), RH_i (in percent), and X_{AirQi} are the temperature, relative humidity, and air quality index associated with the network sensing nodes i = 1,...,4).

The values of V _pal have been experimentally determined for an indoor laboratory wherein a mimic field condition and several simulation experiments of pollution events took place. Thus, values of 1.2–1.7 V have been taken for V _pal while using the Figaro TGS800 inside in clear air. As discussed above, while monitoring the V _AirQ of the captured voltage was used to determine the air quality index the XAirQ. Fig. 10 shows the development of XAirQ for some kinds of pollution events.

Each hyperlink corresponds to a sensing node URL (e.g., http://193.136.143.205/74_sens2.htm), and upon selection, a detailed air quality measurement page is displayed (Fig. 11).

The HTML META tag sets the refresh rate of the webpage to a value in the time interval of 5–60 s according to the air dynamics as follows: META HTTP-EQUIV="refresh" CONTENT="20".

Whenever there is a pollution event in the region for whose air quality page is given below, the alert message "Pollution event on SNj" is issued. Then the operator can click on the associated button "measurement details" of the alert message to request from the Web server the detailed information, namely gas concentration levels (methane, CO, and solvent vapors in this paper).

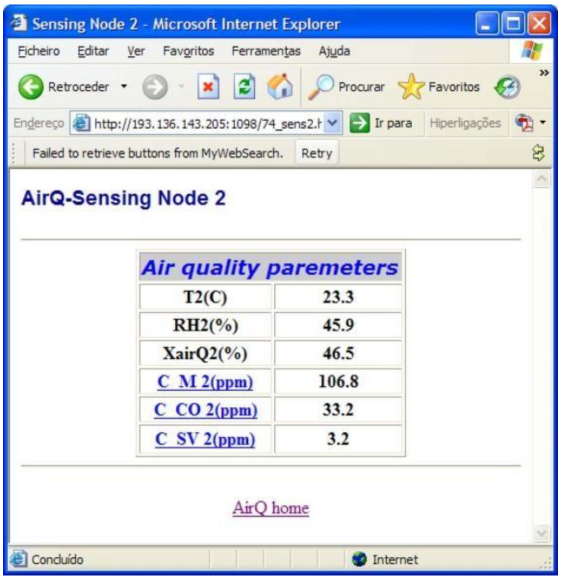

Further "pollution pages" are connected to the measuring gas sensor channels whose hyperlinks are designated in Fig. 11 by C_M, C_CO, and C_SV. Those pages contain the voltage values of the given channel, say VC_M, and its concentration value, say C_M, obtained from processing the NN, and also the temperature and humidity measurements on the SNj level. In order to prevent false alarms due to anomalous functioning of the considered gas concentration measuring channel, values obtained from general air contaminant channel (AC channel) are used. Anomalous situations such as temperature and relative humidity that are out of range for the considered monitored region, e.g., T = 60 ◦C and RH = 0%, and false pollution alarms expressed in high).

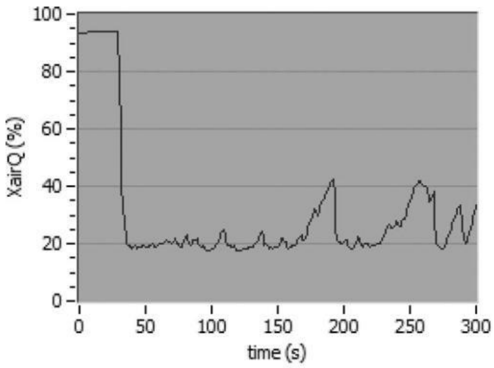

(a)

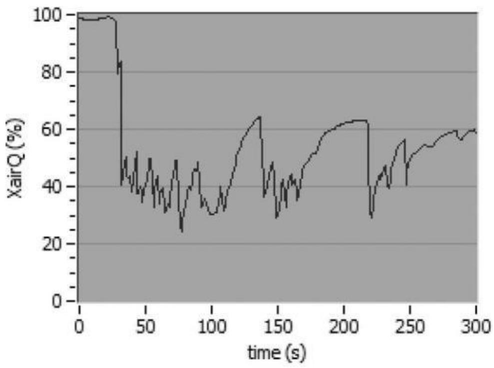

(b)

Fig. 11. Detailed air quality monitoring page—sensing node 2. T_2: Temperature value (in degrees Celsius). RH_2: Humidity values (in percent). X_{AirQ2}: Air quality index (in percent). *C_M*: Methane concentration. *C*_CO: CO concentration. *C*_SV: Solvent vapors concentration.

Concentration values produced by selective gas sensors, like CM = 325 ppm, in case the sensor AC sends a low concentration value, say 10 ppm, in relation to the same measured air.

B. APC LabVIEW Web Server Publishing

Above this, communication was implemented through TCP/IP function in LabVIEW to perform tasks such as advanced data processing and data logging by being based on TCP/IP communication. Making use of the LabVIEW software executed in the PC, it fetches VGsi values from sensing nodes SNj, processes and writes down data to the data logging files, enabling us to obtain the historical evolution of air quality in monitored areas and to evaluate the trends of air quality. Fig. 12 Graphical User Interface (GUI) corresponding to the channel monitoring of SNi.

As seen from the figure, in addition to the output voltage levels concerning the air quality sensors, T, and relative humidity values, pollution events are

signalled once the output voltage of ITGS800 exceeds
the set alarm threshold 4.7 V of this paper
Fig. 10. Evolution of X_{AirQ} index for two home air pollution events. corresponding to 10 ppm of ethanol. On the
(a) Ethanol vapors pollution. (b) Smoke pollution.
configuration panel of SNi elements of IP address and

port are represented.

The interface implemented allows verification of

laptop PC–SNi network communication using the

ping function.

VI. POWER REQUIREMENTS

To characterize the power required by the wireless network for air quality monitoring, a general- purpose-interface-bus-based virtual system was developed that included a set of Agilent 34401A multimeters to evaluate the dissipated power through measurement of current and voltage at SNi, GSji, and WBi levels.

A. **SNi and GSji Power Dissipation**

The SNi power dissipation evaluation was performed with respect to the different measurement activities and active sensors counts. Thus, under normal conditions that is, no pollution event occurred, only temperature, relative humidity, and air quality sensors are active. SNi−GSji

Fig. 13. SNi and GSji current and power consumption (Ic and Pc) over time for a main webpage refresh rate of 5 s. associated power consumption is PSN_GSji = 2.05 W for a voltage supply Vs = +9 V.

The second set of measurements deals with the SNi−GSji power dissipation for different operating conditions, like continuous acquisition with Web publishing and continuous acquisition with TCP/IP data communication based on LabVIEW. Some results are shown in Fig. 13.

As it can be seen from Fig. 13, assuming an air quality webpage refresh rate trefresh = 5 s, the fluctuation of the consumed power Pc = PSNi + PGSji is about 59 mW. Such fluctuation can be associated with data acquisition and dynamic webpage publishing. When the SNi only gets sensor channel voltages and transmits them to the laptop PC by IEEE803.11b through the DWL-810+ wireless bridge to be processed and published by the LabVIEW Web server features, the average power consumption PC-PC is about 98% of PC. Therefore, from that point of view, both web page presentation solutions are equal in the sense of power consumption.

The used gas sensors are big power consumers of the analyzed network. Therefore, with general air monitoring mode of nonpollution event while only TGS800, temperature, and relative humidity sensors are turned on, the average corresponds to the PSN_GSji value mentioned above. Inducing a pollution event, for example, 400 ppm ethanol, the power consumption associated with air quality sensor is shown in Fig. 14.

Once the general air quality sensor detects a pollution event, all the gas sensors of the SNi are activated, which consumes approximately 4 × 1.24 W GSji power. The GSji power consumption is part of the total power consumption that includes the SNi and WBi consumption.

B.WBiPower Dissipation

The major consumer of power during operation of the system is through wireless communication. On a power-on active state mode, the used average power dissipation for wireless bridge is approximately 3.14
W. As long as the link that connects SNi and WBi is

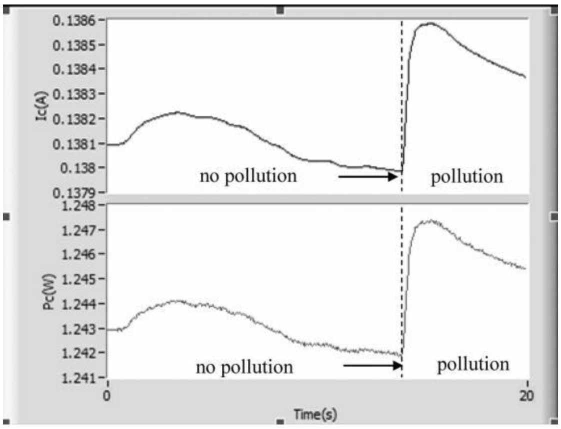

Fig. 14TGS800 power consumption with and without a pollution event.

established, P_{WB_i} reaches 3.58 W. This value is due to the TCP/IP communication between the SN_i and the laptop PC through the implemented WLAN.

VII. CONCLUSION

This paper reports the implementation of a measuring system for air quality monitoring. Two architectures are proposed for wireless communication between the sensing nodes and a personal computer that manages the whole system. Because of the communication range of the hardware used, the systems are particularly suited for indoor applications. The outdoor range limitation can be overcome using high-gain omnidirectional antennas, such as D-Link ANT24-1500, providing extended coverage for an existing 802.11b/g wireless network without the cost and complexity of adding additional wireless APs or wireless repeaters. Coverage of the Wi-Fi designed network can be extended to tens of kilometers by including in the system extended coverage Wi-Fi repeaters, such as Duganit WL-2410.

With the increasing number of low-cost or even free Wi-Fi Internet hotspots and the capabilities of the distributed air-quality-developed system (based on air-quality-embedded Web sensors), different locations can be monitored and the air quality values Web published as long as they have Wi-Fi coverage.

The output of the used gas sensors depends not only on the cross influence of the primary measured gas but also on external influence factors, namely temperature and humidity. Thus, several NPBs were implemented to obtain the temperature and humidity corrected values of the gases' concentrations. The merits of this type of technique for the required purpose, that is the accurate inverse modeling of the gas measuring channel for a small number of calibration points, are well established.

The main novelties of this paper are presented as follows: 1) the development of a wireless network based air quality monitoring system using smart sensors; 2) embedding neural network processing blocks which distribute the charge of the processing between an embedded systems (Web sensor) and the Web browser installed on a personal computer; and 3) PC software for remote TCP/IP controlling of the sensing node with advanced data processing, storing, and the Web-publishing associated software with an air quality monitoring system. Special emphasis was laid on the best deployment of the neural network and on the practical assessment of the power consumption of the distributed sensing system.

Advantages of the proposed air quality monitoring system based on a wireless smart sensor network and on neural network processing blocks embedded on the sensing nodes' HTML pages: • It provides extra capabilities for the air quality monitoring for indoor and outdoor conditions.

•\tIt makes good accuracy of gas concentration measurements by compensating the temperature and humidity influences using neural networks. •\tIt describes a client-side JavaScript solution for neural network implementation.

•\tIt is based on TCP/IP read and write functions implemented in LabVIEW, allowing the advanced processing of air quality data by a PC.

The power requirements of the system, measured for each node, are about 8 W. It is thus clear that only if recharge capabilities of the batteries are included, by means of, for example, solar panels, will a system's autonomy reach days or months.

The output of a specific tin dioxide sensor arrays depends not only on temperature and humidity but also on the concentration of other gases and vapors. The effect of this cross influence on the accuracy of the measurement can be minimized using also neural networks. We will address this problem in a future work.

REFERENCES

[1] European Environment Agency, *Air Pollution*, 2001. Report.

[2] J. Bartolomeo, "Detecting CO in the home," *Home Automation and Building Control*, pp. 51–55, Oct. 1995.

[3] F. Sarry and M. Lumbreras, "Gas discrimination in an airconditioned system," *IEEE Trans. Instrum. Meas.*, vol. 49, no. 4, pp. 809–812, Aug. 2000.

[4] S. Marco, A. Ortega, A. Pardo, and J. Samitier, "Gas identification with tin oxide sensor array and selforganizing maps: Adaptive correction of sensor drifts," *IEEE Trans. Instrum. Meas.*, vol. 47, no. 1, pp. 316–320, Feb. 1998.

[5] A. Lee and B. Reedy, "Temperature modulation in semiconductor gas sensing," *Sens. Actuators B, Chem.*, vol. 60, no. 1, pp. 35–42, Nov. 2, 1999.

[6] F. Ménil, M. Susbielles, H. Debéda, C. Lucat, and P. Tardy, "Evidence of a correlation between the nonlinearity of chemical sensors and the asymmetry of their response and recovery curves," *Sens. Actuators B, Chem.*, vol. 106, no. 1, pp. 407–423, Apr. 29, 2005.

[7] R. Selmic and F. L. Lewis, "Neural-network approximation of piecewise continuous functions:
Application to friction compensation," *IEEE Trans. Neural Netw.*, vol. 13, no. 3, pp. 745–751, May 2002.

[8] H. G. Ramos, J. M. Dias Pereira, V. Viegas, O. Postolache, and P. M. B. Silva Girão, "A virtual instrument to test smart transducer interface modules (STIMs)," *IEEE Trans. Instrum. Meas.*, vol. 53, no. 4, pp. 1232–1239, Aug. 2004.

[9] *IEEE Std. 1451.2-1997, Standard for a Smart Transducer Interface for Sensors and Actuators—Transducer to Microprocessor Communication Protocols and Transducer Electronic Data Sheet (TEDS) Formats*, Sep. 25, 1998, New York: IEEE. #SH94566.

[10] J. M. Dias Pereira, P. M. B. Silva Girão, and O. Postolache, "Fitting transducer characteristics to measured data," *IEEE Signal Process. Mag.*, vol. 4, no. 4, pp. 26–39, Dec. 2001.

[11] J. M. Dias Pereira, P. M. B. Silva Girão, and O. Postolache, "Fitting transducer characteristics to measured data," *IEEE Signal Process. Mag.*, vol. 4, no. 4, pp. 26–39, Dec. 2001.

[12] M. Gast and M. S. Gast, *802.11 Wireless Networks: The Definitive Guide*. Sebastopol, CA: O'Reilly, 2002.

[13] *Gas Sensors Catalog*, Figaro, Osaka, Japan. [Online]. Available:

http://www.figaro.co.jp/en/make_html/item_1.html [14] Smartec, *Smartec-Sensors Catalog*. [Online]. Available: http://www. mmselectronics.co.uk/smt160-30.htm [15] *Relative Humidity Sensor-HS1100*, Humirel Inc., Chandler, AZ, 1999.

[16] J. Patra, A. Kot, and G. Panda, "An intelligent pressure sensor using neural networks," *IEEE Trans. Instrum. Meas.*, vol. 49, no. 4, pp. 829–834, Aug. 2000.